

Kondo disorder and non-Fermi-liquid behavior in $\text{UCu}_{5-x}\text{Pd}_x$ and $\text{CeCu}_{5.9}\text{Au}_{0.1}$

O. O. Bernal* and D. E. MacLaughlin

Department of Physics, University of California, Riverside, California 92521-0413

A. Amato, R. Feyerherm, F. N. Gygax, and A. Schenck

Institute for Particle Physics, Eidgenössische Technische Hochschule-Zürich, CH-5232 Villigen PSI, Switzerland

R. H. Heffner and L. P. Le

Mail Stop K764, Los Alamos National Laboratory, Los Alamos, New Mexico 87545

G. J. Nieuwenhuys

Kamerlingh Onnes Laboratorium, Rijksuniversiteit Leiden, 2300 RA Leiden, The Netherlands

B. Andraka

Department of Physics, University of Florida, Gainesville, Florida 32611

H. v. Löhneysen and O. Stockert

Physikalisches Institut, Universität Karlsruhe, D-76128 Karlsruhe, Germany

H. R. Ott

Laboratorium für Festkörperphysik, Eidgenössische Technische Hochschule-Hönggerberg, CH-8903 Zürich, Switzerland

(Received 22 April 1996; revised manuscript received 24 July 1996)

Muon spin rotation (μSR) has been used to probe non-Fermi-liquid (NFL) behavior in the heavy-fermion alloys $\text{UCu}_{5-x}\text{Pd}_x$, $x=1.0$ and 1.5 , and $\text{CeCu}_{5.9}\text{Au}_{0.1}$. Zero-field μSR puts an upper bound of $\sim 0.01\mu_B/U$ atom on any static magnetism in $\text{UCu}_{5-x}\text{Pd}_x$, which is too weak to affect the transverse-field μSR linewidth or to give rise to NFL behavior. In agreement with NMR results, μSR spectra in transverse fields suggest that a broad distribution of Kondo temperatures (“Kondo disorder”) is important in $\text{UCu}_{5-x}\text{Pd}_x$. NFL anomalies at temperature T then arise from “free” spins for which $T_K \ll T$. Comparison of μSR and NMR linewidths also indicates short-range spatial correlation of the Kondo disorder in $\text{UCu}_{5-x}\text{Pd}_x$, in agreement with the local character of the dynamic susceptibility inferred from neutron scattering experiments. In $\text{CeCu}_{5.9}\text{Au}_{0.1}$ the data suggest significant Kondo disorder only if the spatial correlation is long ranged, which is not indicated by other properties of this alloy. [S0163-1829(96)08141-6]

I. INTRODUCTION

Thermodynamic and transport measurements in a number of heavy-fermion alloys indicate that the Fermi-liquid description appropriate to a conventional spin-singlet Kondo system does not apply to these materials. Perhaps the most striking non-Fermi-liquid (NFL) anomalies are a linear temperature dependence of the resistivity and a logarithmic divergence of the Sommerfeld coefficient $C(T)/T$, where $C(T)$ is the specific heat. Both of these properties characterize nearly every NFL heavy-fermion system discovered to date. The origin of these phenomena is controversial. One school of thought^{1,2} interprets them as arising from a multi-channel quadrupolar or other Kondo mechanism. Another view^{3,4} invokes a zero-temperature quantum critical point, which yields qualitatively different critical phenomena than for a finite critical temperature. It has also been noted⁵ that a distribution of single-spin Kondo temperatures T_K due to structural disorder mimics NFL behavior if the distribution function $P(T_K)$ is broad, i.e., if $T \gg T_K$ for a significant fraction of spins even at low temperatures.

We have carried out positive-muon (μ^+) spin rotation and

relaxation (μSR) studies of two NFL systems, $\text{UCu}_{5-x}\text{Pd}_x$, $x=1.0$ and 1.5 (Ref. 6), and $\text{CeCu}_{5.9}\text{Au}_{0.1}$ (Ref. 7). In these experiments muons are resonant probes of their magnetic environment,⁸ similar to nuclei in nuclear magnetic resonance (NMR). One object of this work was to determine if magnetic freezing, with or without long-range order, occurs in $\text{UCu}_{5-x}\text{Pd}_x$, since this could affect bulk properties and since all NFL systems discovered to date are alloys in which chemical substitution has suppressed a magnetic phase transition. μSR is an ideal tool for this purpose. It is a local probe which is extremely sensitive to static magnetism and its distribution. Unlike Bragg scattering, μSR does not require long-range order for this purpose; unlike NMR, an applied static field is not necessary for μSR . The latter feature turns out to enhance considerably the sensitivity of μSR to weak static magnetism (small or very dilute moments). Our zero-field μSR spectra in $\text{UCu}_{5-x}\text{Pd}_x$ place an upper bound of $\sim 0.01\mu_B/U$ atom on any static magnetism, and we find no evidence for any effect of spin freezing on NFL behavior in $\text{UCu}_{5-x}\text{Pd}_x$. Zero-field μSR studies of the NFL alloys $\text{Y}_{0.8}\text{U}_{0.2}\text{Pd}_3$ (Ref. 9) and $\text{CeCu}_{5.9}\text{Au}_{0.1}$ (Ref. 10) also indicate the absence of static magnetism, so that in NFL systems

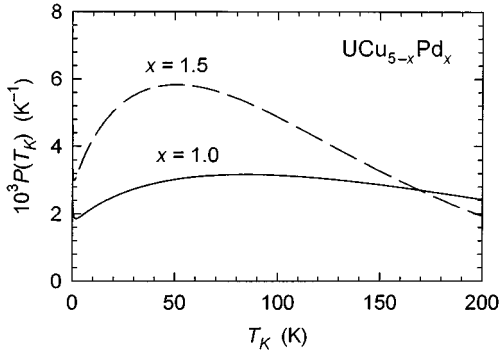


FIG. 1. Distribution function $P(T_K)$ of Kondo temperatures T_K in $\text{UCu}_{5-x}\text{Pd}_x$, $x=1.0$ (solid curve) and 1.5 (dashed curve). From data and analysis of Ref. 11.

studied to date the NFL behavior is not due to spin freezing.

A second object was to elucidate the importance of ‘‘Kondo disorder’’ (the third mechanism enumerated above) by determining the distribution of the local magnetic susceptibility χ . A previous NMR study of $\text{UCu}_{5-x}\text{Pd}_x$ (Ref. 11) revealed strong broadening of the Cu NMR line at low temperatures due to a broad inhomogeneous distribution $P(\chi)$ of χ . The susceptibility of Kondo ions approximately obeys a Curie-Weiss law

$$\chi(T) = C/(T + \theta), \quad (1)$$

where C is the Curie constant and $\theta \approx T_K$ to within a factor of order unity. The observed distribution of χ can therefore be interpreted as due to a corresponding distribution $P(T_K)$ of T_K . This Kondo disorder explained much of the NFL behavior of the bulk susceptibility and specific heat.¹¹ Figure 1 shows the resulting $P(T_K)$ for both Pd concentrations; it can be seen that the Kondo temperatures are widely distributed and that $P(T_K=0) \neq 0$.¹² A recent theoretical treatment of Kondo disorder by Miranda *et al.*¹³ has explained this wide distribution by concluding that correlation effects strongly enhance any extrinsic disorder. Their picture also reproduces the linear temperature dependence of the resistivity, a feature that has eluded other models of NFL behavior.

In $\text{UCu}_{5-x}\text{Pd}_x$ our μSR data confirm the NMR results, thereby corroborating the NMR evidence for Kondo disorder. Comparison of μSR and NMR linewidths yields the additional information that the spatial correlation length ξ which characterizes the disordered static susceptibility is local, i.e., comparable to or shorter than an atomic length scale. This locality of the static susceptibility in $\text{UCu}_{5-x}\text{Pd}_x$ agrees with the local nature of the dynamic susceptibility determined by inelastic neutron scattering (INS).¹⁴

The temperature dependence of the linewidth could be viewed as merely establishing the presence of disorder in the Curie-Weiss temperature θ , which might be due to disorder in properties other than T_K such as crystal-field splitting of the U multiplet or exchange coupling between U spins. But in $\text{UCu}_{5-x}\text{Pd}_x$ there is no sign of crystal-field levels in the INS spectra,¹⁴ and no appreciable static magnetism for temperatures $T \ll \langle \theta \rangle$ (see Sec. III below). Thus the most likely origin of the disordered susceptibility in this system is a distribution of Kondo temperatures, a conclusion which is

further corroborated by the good agreement with experiment of the specific heat calculated in the Kondo disorder model.¹¹

Long-range antiferromagnetic order is found in $\text{CeCu}_{6-x}\text{Au}_x$ above a critical concentration $x \approx 0.1$, whereas pure CeCu_6 does not exhibit magnetic order. For $\text{CeCu}_{5.9}\text{Au}_{0.1}$, i.e., at the critical concentration, NFL behavior has been particularly well established.⁷ This alloy is therefore a very good candidate for a $T=0$ quantum phase transition. Nevertheless, the possibility of Kondo disorder must also be considered in this case. The question of whether or not $P(T_K)$ can account for the NFL properties of $\text{CeCu}_{5.9}\text{Au}_{0.1}$ turns out to depend on the correlation length ξ which characterizes the disordered susceptibility. If ξ is short, as in $\text{UCu}_{5-x}\text{Pd}_x$, then $P(\chi)$ and $P(T_K)$ in $\text{CeCu}_{5.9}\text{Au}_{0.1}$ are found to be narrow, and Kondo disorder is ruled out as the dominant mechanism for NFL behavior. If on the other hand ξ is long, the opposite conclusion follows; the width of $P(\chi)$ is close to that predicted from the Kondo disorder model, and again Kondo disorder can account for much of the NFL behavior. Although ξ cannot be independently determined in this case a number of arguments, to be given below, are in favor of a short ξ , and support the proximity of a magnetic instability as the cause of NFL behavior in $\text{CeCu}_{5.9}\text{Au}_{0.1}$.

II. EXPERIMENTAL TECHNIQUE

Our μSR experiments were carried out at the General Purpose Spectrometer and Low Temperature Facilities on the $\pi\text{M}3$ beam line of the 600-MeV proton accelerator at the Paul Scherrer Institute, Villigen, Switzerland. The $\text{UCu}_{5-x}\text{Pd}_x$ samples consisted of the powders previously used for NMR experiments,¹¹ which were pressed into cylindrical pellets. The $\text{CeCu}_{5.9}\text{Au}_{0.1}$ single crystal, previously used in a μSR search for static magnetism,¹⁰ was oriented with the c axis (orthorhombic notation) parallel to the applied field and the muon beam. The susceptibility data below 6 K were taken with a moving-sample magnetometer in an applied field of 1 kOe parallel to the c axis, and data between 4 and 300 K were taken using a superconducting quantum interference device magnetometer in a field of 10 Oe, again with $\mathbf{H} \parallel c$. Agreement was excellent in the temperature range of overlap.

Most μSR spectra were obtained in zero field and in a transverse field¹⁵ of 5 kOe. Although the susceptibility and μSR linewidths were measured in different fields, the former is not expected to depend significantly on field for $H \lesssim 5$ kOe. A few measurements were made in small longitudinal fields; in this case only dynamic fluctuations contribute to the μ^+ relaxation rate.¹⁶ These longitudinal-field spectra showed no evidence for significant dynamic relaxation in $\text{UCu}_{5-x}\text{Pd}_x$ at any temperature.

III. ZERO-FIELD μSR

The zero-field μ^+ relaxation data are best described by a Kubo-Toyabe function¹⁶ at low temperatures, corresponding to a Gaussian distribution of static μ^+ local fields H_L . As shown in Fig. 2(a), there are no ‘‘wiggles’’ or other signs of strong static magnetism in the asymmetry spectra. Figure 2(b) gives the Kubo-Toyabe relaxation rate $\sigma_{\text{KT}}(T)$ in

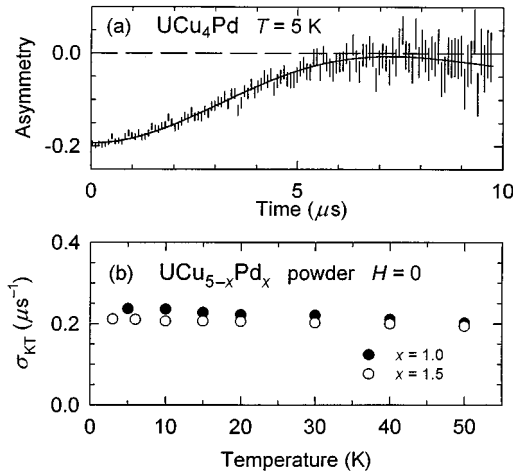


FIG. 2. (a) Data points: zero-field μ SR asymmetry spectrum in UCu_4Pd . Curve: fit to Kubo-Toyabe relaxation function. (b) Temperature dependence of zero-field μ^+ Kubo-Toyabe relaxation rate σ_{KT} in $\text{UCu}_{5-x}\text{Pd}_x$, $x=1.0$ and 1.5 .

$\text{UCu}_{5-x}\text{Pd}_x$, $x=1.0$ and 1.5 , the values of which correspond to rms widths of 2–3 Oe. Given that the μ^+ dipolar field due to neighboring (mainly Cu) nuclei is also of this order of magnitude, a conservative upper bound on the field due to static U magnetism is $(\delta H_L)_{\text{rms}} \approx 1$ Oe.

We estimate the corresponding static U moment by assuming for definiteness the U spins freeze in the antiferromagnetic structure found by neutron scattering in the end compound UCu_5 ,¹⁷ and that the U spins are coupled to muon spins via the dipolar interaction. Then the measured value of $(\delta H_L)_{\text{rms}}$ corresponds to a very small static U moment ($\leq 0.01 \mu_B/U$ atom), a conclusion which is likely to hold roughly for any other frozen magnetic configuration. The slight dependence of σ_{KT} on temperature and x in Fig. 2(b) may indicate weak spin freezing, with either a small U moment ($\leq 0.01 \mu_B/U$ atom) or a small concentration ($\leq 1\%$) of paramagnetic impurities.

This small upper bound on any static magnetism in $\text{UCu}_{5-x}\text{Pd}_x$ has two important consequences. First, the limit on the static U moment is an order of magnitude smaller than the value needed to account for either the Cu NMR linewidths in $\text{UCu}_{5-x}\text{Pd}_x$ (Ref. 18) or the μ SR linewidths reported in this paper. The observed broadening must therefore be due to paramagnetism, i.e., to a distribution of Knight shifts. Second, an interpretation of the observed thermodynamic and transport NFL behavior as unrecognized consequences of spin freezing is ruled out by the small upper bound.

IV. KONDO DISORDER AND NFL BEHAVIOR

If the distribution function $P(T_K)$ is broad enough so that $P(T_K=0) \neq 0$, i.e., that there is a finite number of Kondo spins with $T_K < T$ at any finite temperature T , then we can think of the Kondo singlet state as broken up for these spins: they become “free,” dominate the low-temperature thermodynamics and transport properties, and are capable of giving rise to NFL behavior. In the Kondo-disorder model the magnetization $M(H, T)$ of the low- T_K free spins approximately follows a Brillouin function, and saturates in a sufficiently

strong magnetic field $H \gg k_B T / \mu_B$. This leads to a field dependence of the sample-averaged or bulk magnetic susceptibility $\langle \chi(H, T) \rangle = \langle M(H, T) \rangle / H$.

In Ref. 11 this picture is taken further by constructing a simple model of Kondo disorder from a microscopic point of view. The Kondo temperature is given roughly by

$$T_K = E_F \exp(-1/\lambda),$$

where E_F is the Fermi energy and $\lambda = \rho \mathcal{J}$ is the Kondo coupling constant; here ρ is the density of conduction-band states at the Fermi energy and \mathcal{J} is the conduction-electron–Kondo-ion exchange constant. Even modest disorder in either ρ or \mathcal{J} produces considerable disorder in T_K , thanks to the amplifying effect of the exponential dependence for small λ . We assume a relatively narrow Gaussian distribution function $P(\lambda)$ for the distribution of λ ; as shown below we find widths $w = (\delta \lambda)_{\text{rms}}$ of the order of 20% of the mean $\langle \lambda \rangle$ in $\text{UCu}_{5-x}\text{Pd}_x$ for $x=1.0$ and 1.5 .

For these alloys the resulting distribution functions $P(T_K) = |d\lambda/dT_K| P(\lambda)$, shown in Fig. 1, are quite broad, and $P(T_K=0) \neq 0$ as required to obtain asymptotic NFL behavior. For comparison with experiment we wish to calculate the average and rms width of the susceptibility distribution. The general n th moment is given by

$$\begin{aligned} \langle [\chi(H, T)]^n \rangle &= \int d^3r [\chi(\mathbf{r})]^n \\ &= \int_0^\infty dT_K P(T_K) [\chi(H, T; T_K)]^n, \end{aligned}$$

and we make a crude representation of the single-ion Kondo physics by writing the susceptibility $\chi(H, T; T_K) = M(H, T; T_K) / H$ as

$$\chi(H, T; T_K) = g \mu_B J B_J(x) / H.$$

Here $B_J(x)$ is the Brillouin function for free spins of angular momentum J , and

$$x = \frac{g \mu_B J H}{k_B (T + \alpha T_K)}.$$

This preserves the approximate Curie-Weiss form of the Kondo susceptibility, and also allows low-temperature saturation of spins with small T_K .

Our analysis of Kondo disorder proceeds as follows.¹¹ We first obtain the parameters of $P(T_K)$ [mean and width of the distribution of $P(\lambda)$] by fitting the bulk average susceptibility (first moment) $\langle \chi(H, T) \rangle$ to the experimental data. The field dependence of χ gives the needed sensitivity to the width of $P(\lambda)$. [We note that the magnetic susceptibility was measured before and after grinding the sample into a powder and found to be unchanged; any modification of $P(T_K)$ due to disorder introduced by the grinding is therefore negligible.] Once we have defined $P(T_K)$ we can calculate the rms width $(\delta \chi)_{\text{rms}} = (\langle \chi^2 \rangle - \langle \chi \rangle^2)^{1/2}$ with no further adjustable parameters. This theoretical width can then be compared with estimates of $(\delta \chi)_{\text{rms}}$ obtained from NMR and μ SR linewidths as described in the next section.

V. TRANSVERSE-FIELD μ SR; SUSCEPTIBILITY INHOMOGENEITY

A. Relation between μ SR/NMR linewidth and susceptibility distribution

To obtain information on the disordered susceptibility from the transverse-field μ SR and NMR spectra we must consider the manner in which this disorder is reflected in the spin-probe resonance linewidths. In general the dipolar and transferred hyperfine (thf) couplings between local moments¹⁹ and a spin probe (μ^+ or nuclear spin) at site i lead to a relative frequency shift K_i given by

$$K_i = \sum_j a_{ij} \chi_j, \quad (2)$$

where χ_j is the susceptibility of the j th moment and a_{ij} is proportional to the local field generated at site i by a unit local moment at site j . Thus the distribution of frequency shifts $P(K)$ reflects the distribution of local-moment susceptibilities $P(\chi)$, assuming for the moment that a_{ij} is the same for crystallographically equivalent values of i and j ; disorder in a_{ij} will be considered separately. From Eq. (2) we construct the spatial averages

$$\langle K \rangle = a \langle \chi \rangle, \quad a \equiv \sum_j a_{ij}$$

and

$$\kappa^2 \equiv \langle \delta K^2 \rangle = \sum_{jk} a_{ij} a_{ik} \langle \delta \chi_j \delta \chi_k \rangle. \quad (3)$$

Here the coupling constant a is independent of i in an ordered lattice, and $\delta K = K - \langle K \rangle$ and $\delta \chi = \chi - \langle \chi \rangle$ are the deviations of the shift and susceptibility, respectively, from their averages. Thus the rms width κ depends on the correlation function $\langle \delta \chi_j \delta \chi_k \rangle$, and in particular on the correlation length ξ which characterizes it.

There are two extreme limits. In the limit of long-range correlation (LRC) the susceptibility is disordered in macroscopic domains, i.e., ξ is much longer than the local-moment near-neighbor spacing. Then each spin probe senses a locally uniform susceptibility, so that $\langle \delta \chi_j \delta \chi_k \rangle \approx \langle \delta \chi^2 \rangle$ may be factored out of the summation in Eq. (3). This yields

$$\kappa^2 = a^2 \langle \delta \chi^2 \rangle \quad (\text{LRC}),$$

so that

$$\kappa = |a| (\delta \chi)_{\text{rms}} \quad (\text{LRC}),$$

and the fractional width $(\delta \chi)_{\text{rms}} / \langle \chi \rangle$ is

$$(\delta \chi)_{\text{rms}} / \langle \chi \rangle = \kappa / (a^* \langle \chi \rangle) \quad (4)$$

with

$$a^* = a_{\text{LRC}}^* = |a| = \left| \sum_j a_{ij} \right|. \quad (5)$$

This limit was implicitly assumed in Ref. 11 but, as we shall see, is incorrect in the case of $\text{UCu}_{5-x}\text{Pd}_x$.

In the extreme opposite limit of short-range correlation (SRC) ξ is much shorter than the moment spacing, i.e., the variation of χ_j from site to site is random.²⁰ Then

$$\langle \delta \chi_j \delta \chi_k \rangle = \begin{cases} \langle \delta \chi^2 \rangle, & j=k, \\ 0, & j \neq k \end{cases} \quad (\text{SRC}).$$

In this case one finds

$$\kappa^2 = \sum_j a_{ij}^2 \langle \delta \chi^2 \rangle \quad (\text{SRC}),$$

so that again $(\delta \chi)_{\text{rms}} / \langle \chi \rangle = \kappa / (a^* \langle \chi \rangle)$, but with

$$a^* = a_{\text{SRC}}^* = \left(\sum_j a_{ij}^2 \right)^{1/2}. \quad (6)$$

Clearly a_{LRC}^* [Eq. (5)] and a_{SRC}^* [Eq. (6)] can be quite different. In the following we use $\kappa / (a_{\text{LRC}}^* \langle \chi \rangle)$ and $\kappa / (a_{\text{SRC}}^* \langle \chi \rangle)$ as estimates of $(\delta \chi)_{\text{rms}} / \langle \chi \rangle$ in the corresponding limits.

We now consider the case where both χ and the a_{ij} are disordered. Then

$$\langle K \rangle = \sum_j \langle a_{ij} \chi_j \rangle \quad \text{and} \quad \langle K^2 \rangle = \sum_{j,k} \langle a_{ij} a_{ik} \chi_j \chi_k \rangle.$$

It is difficult to go further without assuming that the distributions of a_{ij} and χ are uncorrelated. Making this assumption, one finds that

$$\langle K \rangle = \langle a \rangle \langle \chi \rangle, \quad \langle a \rangle = \sum_j \langle a_{ij} \rangle,$$

and

$$\kappa^2 = \sum_{jk} (\langle \delta a_{ij} \delta a_{ik} \rangle \langle \chi \rangle^2 + \langle a_{ij} a_{ik} \rangle \langle \delta \chi_j \delta \chi_k \rangle). \quad (7)$$

Thus we have a term in $\langle \chi \rangle^2$, with coefficient proportional to the deviations of the coupling constants, in addition to the original term in $\langle \delta \chi_j \delta \chi_k \rangle$.

B. Data analysis and discussion

a. $\text{UCu}_{5-x}\text{Pd}_x$. The transverse-field μ^+ linewidth σ in UCu_4Pd , obtained from fits of the data to a Gaussian line shape, is plotted versus the molar susceptibility in Fig. 3 with temperature an implicit parameter. The measured linewidth contains a contribution from nuclear dipolar fields as well as from coupling to the U moments. The two contributions add in quadrature, since the electronic and nuclear field distributions are uncorrelated. We estimate the nuclear contribution $\sigma_{\text{nuc}} = 0.24 \mu\text{s}^{-1}$ from the low-temperature rate in zero field (Fig. 2), assuming it is independent of temperature. The correction is most important at small susceptibilities (high temperatures), and uncertainty in it would not appreciably affect our conclusions.

The μ^+ linewidth is unambiguously due to a static distribution of local fields, since σ is orders of magnitude larger than the dynamic rate measured in longitudinal applied fields (not shown). The plot of $\sigma(T)$ against $\chi(T)$ in Fig. 3 is motivated by the fact that if χ were uniform, then σ should be proportional to χ . This can be seen by considering Eq. (7) with $\delta \chi_j = 0$, in which case $\sigma = \omega_0 \kappa \langle \chi \rangle$, where ω_0 is the μ^+

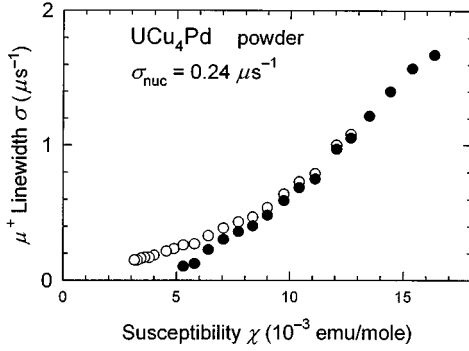


FIG. 3. μ^+ Gaussian linewidth σ vs bulk molar susceptibility in UCu_4Pd , with temperature (range 4–300 K) an implicit parameter, in a transverse field $H_T=5$ kOe. Open circles: measured linewidths. Filled circles: linewidths after correction for nuclear dipole broadening.

Larmor frequency in the applied field. Figure 3 shows that this proportionality is not obeyed for UCu_4Pd .

At the μ^+ stopping sites, which have been identified as the a and c sites (Wyckoff notation) in the parent compound UCu_5 (Ref. 21), the tetrahedral point symmetry ($\bar{4}3m$) implies no net dipolar coupling for uniform U -spin polarization. This point symmetry together with the cubic crystal structure (space group $F43m$) implies a vanishing μ^+ anisotropic Knight shift, so that there is no powder-pattern broadening of the μ^+ line. In addition, in $\text{UCu}_{5-x}\text{Pd}_x$ the measured μ^+ isotropic shift K_{iso} , which can arise only from the isotropic thf coupling constant a_{thf} , is found to be small and not linear in χ . As shown in Fig. 4, a (poor) straight-line fit yields $|a_{\text{thf}}|=|K_{\text{iso}}/\chi|\leq 0.028$ mol/emu for UCu_4Pd , which we take as an upper bound on a_{LRC}^* for this alloy. The average calculated values of a_{SRC}^* [Eq. (6)] in UCu_4Pd , assuming only dipolar coupling, are 0.107 mole/emu for the c site and 0.084 mole/emu for the a site. Thus for a given experimental value of κ the estimate of $(\delta\chi)_{\text{rms}}/\chi$ from Eq. (4) will be considerably larger for the LRC limit (smaller a^*) than for the SRC limit (larger a^*).

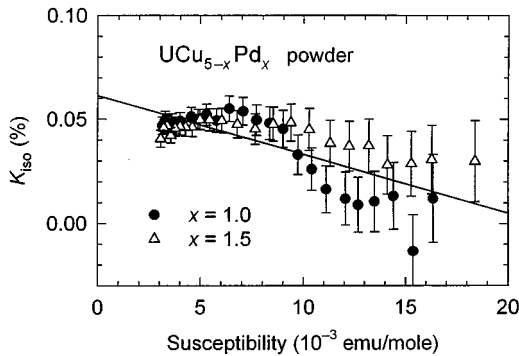


FIG. 4. μ^+ isotropic frequency shift K_{iso} vs bulk molar susceptibility in $\text{UCu}_{5-x}\text{Pd}_x$, $x=1$ (circles) and 1.5 (triangles), $H_T=5$ kOe, temperature range 4–300 K. The weak nonlinear temperature dependence is not understood and may reflect systematic error (e.g., from the fit of a Gaussian line to a temperature-dependent line shape.) The error bars include uncertainty in the Lorentz and demagnetization field corrections. Straight line: linear fit to data for $x=1.0$, used to estimate the coupling constant a (see text).

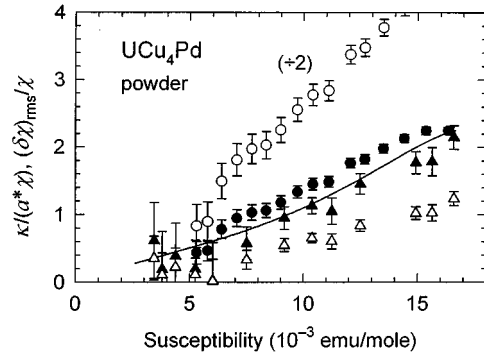


FIG. 5. Estimates of the relative rms width $(\delta\chi)_{\text{rms}}/\chi$ of the susceptibility distribution in UCu_4Pd . Points: normalized relative linewidths $\kappa/(a^*\chi)$ in the LRC (open symbols) and SRC (filled symbols) limits, from μSR (circles) and NMR [triangles (Ref. 11)] linewidths. Curve: relative rms susceptibility $(\delta\chi)_{\text{rms}}/\chi$ from the Kondo-disorder model. Agreement between μSR and NMR estimates in the SRC limit is good, as is agreement with the Kondo-disorder prediction.

For the μSR analysis the dipolar value of a_{SRC}^* was used, since the shift data of Fig. 4 yield only a small correction from the thf coupling. The upper bound on a_{LRC}^* established above was used for the LRC-limit calculation, because the large errors in the shift data render the individual values of $a_{\text{LRC}}^*=|K|/\chi$ too imprecise to be meaningful. As a consequence the μSR data give only a lower limit on $\kappa/(a^*\chi)$ in the LRC limit. In UCu_4Pd the resultant μSR LRC-limit and SRC-limit values of $\kappa/(a^*\chi)$, shown as circles in Fig. 5, differ by at least a factor of 4. The strong χ dependence of $\kappa/(a^*\chi)$ in both limits confirms that a distribution of χ dominates the μSR linewidth in UCu_4Pd .

We can also calculate a^* for the Cu NMR linewidth data of Ref. 11 in both the LRC and SRC limits. As noted above, the values of $\kappa/(a^*\chi)$ in Ref. 11 were obtained in the LRC limit, using the experimental value of the average Knight shift. Here we obtain a_{SRC}^* from a_{LRC}^* using the fact that for Cu nuclei in $\text{UCu}_{5-x}\text{Pd}_x$ $a_{\text{thf}}\gg a_{\text{dip}}$ (Ref. 22) and assuming that nearest-neighbor thf contributions are dominant. From Eqs. (5) and (6), for n nearest neighbors with identical isotropic hf coupling strengths we have

$$a_{\text{LRC}}^*\propto n \quad \text{and} \quad a_{\text{SRC}}^*\propto\sqrt{n},$$

so that

$$a_{\text{SRC}}^*=a_{\text{LRC}}^*/\sqrt{n}.$$

For $x\geq 1$ in $\text{UCu}_{5-x}\text{Pd}_x$ all Cu atoms are on sites with three U nearest neighbors, so we take $a_{\text{SRC}}^*=a_{\text{LRC}}^*/\sqrt{3}$. This procedure yields $(a^*)_{\text{LRC}}^{\text{NMR}}=0.60$ mole/emu and $(a^*)_{\text{SRC}}^{\text{NMR}}=0.35$ mole/emu in both UCu_4Pd and $\text{UCu}_{3.5}\text{Pd}_{1.5}$. The resulting NMR values of $\kappa/(a^*\chi)$ are plotted as triangles in Fig. 5.

We address the question of which correlation limit is appropriate in $\text{UCu}_{5-x}\text{Pd}_x$ by comparing the behavior of $\kappa/(a^*\chi)$ obtained from μSR and NMR (Ref. 11) linewidths in both the SRC and LRC limits. Since the values of a^* are

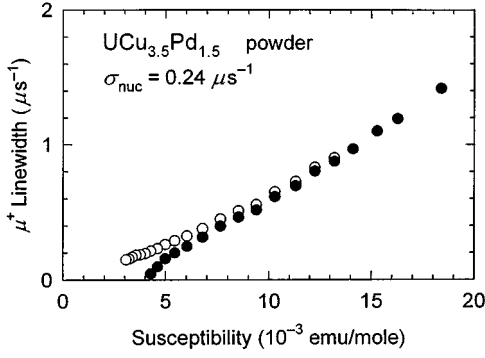


FIG. 6. μ^+ Gaussian linewidth σ vs bulk molar susceptibility in $\text{UCu}_{3.5}\text{Pd}_{1.5}$, with temperature an implicit parameter, $H_T=5$ kOe, temperature range 4–300 K. Open circles: measured linewidths. Filled circles: linewidths after correction for nuclear dipole broadening.

different for μSR and NMR and also for the two correlation limits, agreement between μSR and NMR estimates of $(\delta\chi)_{\text{rms}}/\chi$ is expected only for the correct limit. From Fig. 5 we note that in the SRC limit the agreement between μSR and NMR estimates (filled symbols) is quite good, but in the LRC limit the μSR and NMR data (open symbols) give very different estimates of $(\delta\chi)_{\text{rms}}/\chi$. Furthermore, the LRC-limit μSR value of $\kappa/(a^*\chi)$ (which, we recall, is only a lower bound) is very far from the other three experimental estimates.

These results indicate that the disordered susceptibility in UCu_4Pd is characterized by short-range correlation, a conclusion which, we stress, is independent of the validity of the Kondo-disorder model. But we see in Fig. 5 that the Kondo-disorder calculation of $(\delta\chi)_{\text{rms}}/\chi$ (Ref. 11) (curve), carried out as described in Sec. IV, is in excellent agreement with the $\mu\text{SR}/\text{NMR}$ estimates in the SRC limit. This result is strong evidence that the Kondo-disorder model gives a consistent explanation of the NFL properties of UCu_4Pd .

We next consider the corresponding data from $\text{UCu}_{3.5}\text{Pd}_{1.5}$. Figure 6 gives the measured μ^+ linewidths in this alloy, and the corresponding values of $\kappa/(a^*\chi)$ from μSR and NMR data in both correlation limits are shown in Fig. 7 assuming no inhomogeneity in the a_{ij} . The trends of the data are similar to those in UCu_4Pd , but it can be seen that in the SRC limit the agreement between μSR and NMR values of $\kappa/(a^*\chi)$ (filled symbols) is not as good; the μSR values lie above the NMR values and for $\chi \geq 7 \times 10^{-3}$ emu/mole do not vary as rapidly with χ .

We interpret this to mean that there is a χ -independent contribution to $\kappa/(a^*\chi)$ from disorder in the μ^+ coupling constants a_{ij} in $\text{UCu}_{3.5}\text{Pd}_{1.5}$. We have tested this hypothesis by using a corrected value $(\kappa^2 - (\delta a)_{\text{rms}}^2 \langle \chi \rangle^2)^{1/2}$ [Eq. (7)] in the calculation of $\kappa/(a^*\chi)$ from the μSR data; the result is shown in Fig. 8. It can be seen that excellent agreement between the μSR and NMR values is restored in the SRC limit for the choice $(\delta a)_{\text{rms}}=0.12$ mole/emu, and that the χ dependence of $\kappa/(a^*\chi)$ is again reproduced by the Kondo-disorder model. Thus the same conclusion emerges as in the case of UCu_4Pd , namely, that the μSR and NMR data are in much better agreement with each other in the SRC limit than in the LRC limit.

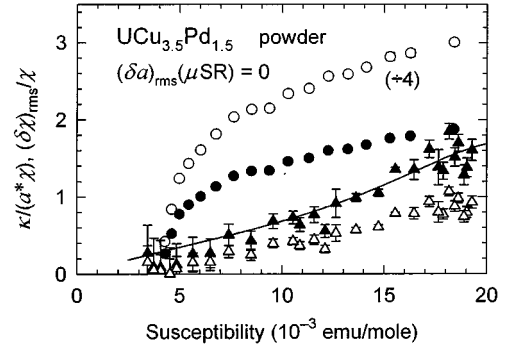


FIG. 7. Estimates of the relative rms width $(\delta\chi)_{\text{rms}}/\chi$ of the susceptibility distribution in $\text{UCu}_{3.5}\text{Pd}_{1.5}$. Points: normalized relative linewidths $\kappa/(a^*\chi)$ in the LRC (open symbols) and SRC (filled symbols) limits, from μSR (circles) and NMR (triangles; data of Ref. 11) linewidths. Curve: relative rms susceptibility $(\delta\chi)_{\text{rms}}/\chi$ from the Kondo disorder model. Agreement between μSR and NMR estimates in the SRC limit is only qualitative.

More disorder was also observed in the Cu NMR quadrupole splitting in $\text{UCu}_{3.5}\text{Pd}_{1.5}$ than in UCu_4Pd (Ref. 11), which can be understood as a result of the tendency of UCu_4Pd to form as an ordered stoichiometric compound. That is, both the quadrupole splitting and $(\delta a)_{\text{rms}}$ reflect this difference in the amount of *structural* (not Kondo) disorder. Note, however, that it is very clear from the behavior of the μSR and NMR linewidths discussed above that the distributions of T_K are broad and comparable in both alloys. In fact $P(T_K)$ is broader in UCu_4Pd than in $\text{UCu}_{3.5}\text{Pd}_{1.5}$ (Fig. 1). The Kondo-disorder theory of Miranda *et al.* may account for this by showing that correlation enhances the effect of the disorder. It is not clear why $(\delta a)_{\text{rms}}$ should be significant in $\text{UCu}_{3.5}\text{Pd}_{1.5}$ for μSR but not for NMR.

b. CeCu_{5.9}Au_{0.1}. In this alloy the μ^+ frequency shift, shown in Fig. 9, is appreciable and varies considerably with the susceptibility. This indicates strong coupling between the μ^+ and Ce spins. The nonlinearity evident in Fig. 9 could be due to any of a number of sources: (1) a temperature-dependent coupling strength, possibly due to thermal popu-

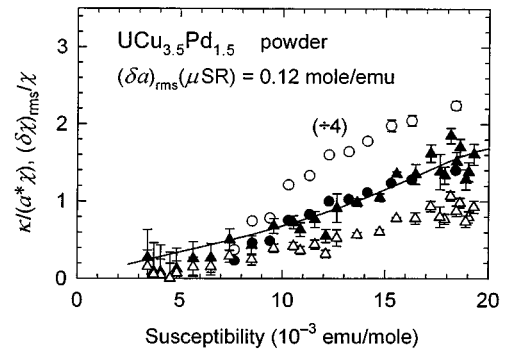


FIG. 8. Same as Fig. 7, but using the corrected form $(\kappa^2 - (\delta a)_{\text{rms}}^2 \langle \chi \rangle^2)^{1/2}$ (circles) for the μSR estimates of $(\delta\chi)_{\text{rms}}/\chi$ (see text). Agreement between μSR and NMR estimates in the SRC limit and with the relative rms susceptibility $(\delta\chi)_{\text{rms}}/\chi$ from the Kondo disorder model (curve) is restored with $(\delta a)_{\text{rms}}=0.12$ mole/emu.

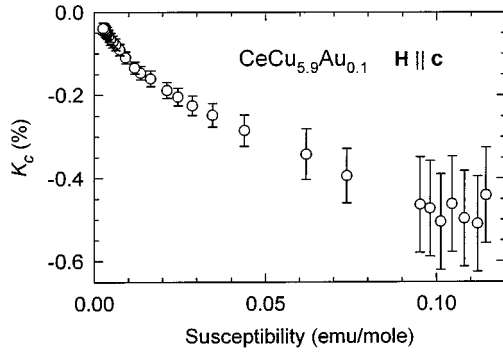


FIG. 9. μ^+ frequency shift K_c in single-crystal $\text{CeCu}_{5.9}\text{Au}_{0.1}$, $\mathbf{H} \parallel \mathbf{c}$ (orthorhombic notation), $H_T=5$ kOe, temperature range 80 mK–300 K. The error bars include uncertainty in the Lorentz and demagnetization field corrections.

lation of Ce^{3+} states split by the crystalline electric field; (2) modification of the local susceptibility by the muon; (3) more than one component of the susceptibility;²³ or (4) muon diffusion at high temperatures (see below); the mechanism is not important to our argument. The μ^+ stopping site, determined in the parent compound CeCu_6 (Ref. 24), has low (1) symmetry and the dipolar coupling does not vanish. Unfortunately no NMR linewidth data are available²⁵ in $\text{CeCu}_{6-x}\text{Au}_x$, so we cannot distinguish directly between the LRC and SRC limits in this system. We have determined the μSR value of a_{LRC}^* using the shift data of Fig. 9, and a_{SRC}^* was calculated using dipolar couplings and the hf interaction (which is a small correction) reported for CeCu_6 in Ref. 24. Again only nearest-neighbor hf coupling was assumed, and the analysis is the same as that of the $\text{UCu}_{5-x}\text{Pd}_x$ μSR and NMR coupling constants described above.

Figure 10 gives the μ^+ linewidths in $\text{CeCu}_{5.9}\text{Au}_{0.1}$, and the calculated dependence of $\kappa/(a^*\chi)$ on χ assuming $(\delta a)_{\text{rms}}=0$ is shown in Fig. 11. These μSR experiments were carried out in a single crystal with $\mathbf{H} \parallel \mathbf{c}$, so that there can be no powder-pattern broadening due to an anisotropic Knight shift; the observed broadening must be due to disorder in either the susceptibility or the hyperfine coupling. The reduction of $\kappa/(a^*\chi)$ for $\chi \leq 0.03$ emu/mole may be due to motional narrowing caused by μ^+ diffusion at high tempera-

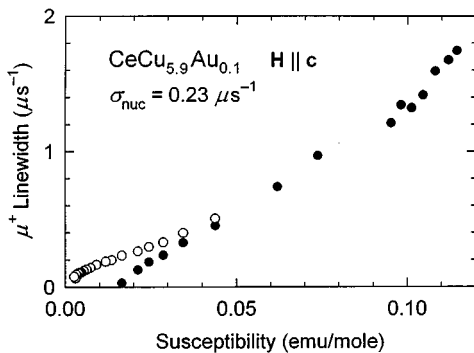


FIG. 10. μ^+ Gaussian linewidth σ vs bulk molar susceptibility in $\text{CeCu}_{5.9}\text{Au}_{0.1}$, $\mathbf{H} \parallel \mathbf{c}$, $H_T=5$ kOe. Open circles: measured linewidths. Filled circles: linewidths after correction for nuclear dipole broadening.

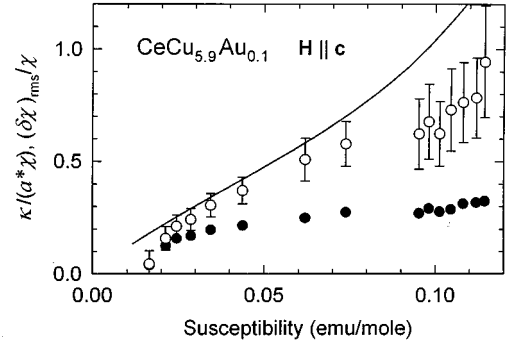


FIG. 11. Estimates of relative rms width $(\delta\chi)_{\text{rms}}/\chi$ of susceptibility distribution in $\text{CeCu}_{5.9}\text{Au}_{0.1}$ (cf. Fig. 5). Points: $\kappa/(a^*\chi)$ in the LRC (open circles) and SRC (filled circles) limits. Curve: relative rms width $(\delta\chi)_{\text{rms}}/\chi$ from the Kondo disorder model.

tures or, alternatively, an effect of nonzero $(\delta a)_{\text{rms}}$ as in $\text{UCu}_{3.5}\text{Pd}_{1.5}$ (Figs. 7 and 8); we do not need to understand this effect in detail for a qualitative discussion, as our conclusions are mainly based on the behavior of the data at large χ .

We see that assuming the SRC limit (filled circles in Fig. 11) yields $\kappa/(a^*\chi)$ an order of magnitude smaller than in UCu_4Pd and, apart from the low- χ dropoff, only a relatively weak variation with χ . This indicates that the assumption of the SRC limit yields a susceptibility distribution which is considerably narrower (although still appreciable), in which case Kondo disorder in $\text{CeCu}_{5.9}\text{Au}_{0.1}$ is not the dominant factor that it is in $\text{UCu}_{5-x}\text{Pd}_x$. If on the other hand the system is in the LRC limit, then $\kappa/(a^*\chi)$ (open circles in Fig. 11) is considerably larger and more temperature dependent.

The SRC limit and its consequences would be in line with the magnetic instability scenario for NFL behavior. Many of the properties of $\text{CeCu}_{6-x}\text{Au}_x$ can be understood²⁶ by assuming a two-component model, where the two components differ in whether or not an Au atom is a near neighbor to a given Ce site. This picture implies short-range correlation of any disorder in χ , arising from the statistical distribution of Au atoms on the Cu(2) sites. Assuming the SRC limit, the lack of strong temperature dependence of $\kappa/(a^*\chi)$ implies that it is dominated by a distribution of coupling constants rather than a distribution of susceptibilities.

In any event $\kappa/(a^*\chi)$ is not large enough to account for the NFL properties of $\text{CeCu}_{5.9}\text{Au}_{0.1}$, as we now proceed to demonstrate. As in $\text{UCu}_{5-x}\text{Pd}_x$ (Ref. 11) we fit the Kondo-disorder model to the field- and temperature-dependent susceptibility of $\text{CeCu}_{5.9}\text{Au}_{0.1}$ (Ref. 7), and use the resultant $P(T_K)$ to calculate $(\delta\chi)_{\text{rms}}/\chi$ with no further adjustable parameters. The result is given by the curve in Fig. 11, where it can be seen that $\kappa/(a^*\chi)$ in the SRC limit lies well below the Kondo-disorder model prediction. The discrepancy is visibly less in the LRC limit, but the SRC limit is believed to be more appropriate to $\text{CeCu}_{5.9}\text{Au}_{0.1}$ for the reasons given above. Moreover, the effect of nonzero $(\delta a)_{\text{rms}}$ would be to reduce the estimated $(\delta\chi)_{\text{rms}}/\chi$ (cf. Figs. 7 and 8) in both limits; this would degrade the agreement between the Kondo-disorder prediction and the LRC-limit estimate. Finally, the different temperature dependences of χ and C/T in $\text{CeCu}_{5.9}\text{Au}_{0.1}$ do not seem to accord with the $\ln T$ behavior of

both these quantities predicted by the theory of Miranda *et al.*¹³ This is also true in $\text{UCu}_{5-x}\text{Pd}_x$, but careful comparisons with experiment must be made in both systems before firm conclusions are drawn.

VI. CONCLUSIONS

These μSR measurements shed light on several issues in NFL heavy-fermion systems. First, significant spatial disorder in the susceptibility is observed in $\text{UCu}_{5-x}\text{Pd}_x$ and, to a lesser extent, in $\text{CeCu}_{5.9}\text{Au}_{0.1}$. It is intriguing that these are both substitutional alloys in which the f lattice is intact. In contrast, in the NFL alloy system $\text{Y}_{1-x}\text{U}_x\text{Pd}_3$, where the f lattice is diluted, the ^{89}Y linewidth varies more slowly than linearly with the susceptibility and gives no evidence for disorder in χ .²⁷ (Here the U ions are substitutionally disordered and the distribution of coupling constants a_{ij} appears to dominate the linewidth.) This regularity can be understood if one assumes that only near-neighbor hybridization between f and non- f ions is important. Such hybridization is not substantially modified by f -lattice dilution, since f ions have only non- f near neighbors, but is affected by disorder in the non- f constituents. Future experiments on both kinds of NFL systems will test this conjecture.

Second, we note that NFL in an ordered compound could not be due to Kondo disorder, but disorder by no means rules out other mechanisms. We have found examples of both Kondo-disorder and “non-Kondo-disorder” NFL alloys ($\text{UCu}_{5-x}\text{Pd}_x$ and $\text{CeCu}_{5.9}\text{Au}_{0.1}$, respectively). We can say no more on the very important question of whether disorder is in fact a necessary condition for NFL behavior; only the discovery of an ordered NFL heavy-fermion (i.e., f -electron)

compound will answer this question conclusively. It should be noted, however, that the ordered d -electron compounds MnSi (Ref. 28) and ZrZn_2 (Ref. 29) exhibit NFL behavior under pressure.

Finally, in $\text{UCu}_{5-x}\text{Pd}_x$ the large μSR linewidth and good agreement between μSR and NMR results in the SRC limit confirm the importance of Kondo disorder in this system, and are strong evidence for weak spatial correlation of the disorder. As noted above, this result and the q -independent INS intensity in $\text{UCu}_{5-x}\text{Pd}_x$ (Ref. 14) taken together indicate that both the static and the dynamic susceptibility are local in nature. In contrast, Kondo disorder is considerably less important in $\text{CeCu}_{5.9}\text{Au}_{0.1}$ if, as suggested by other experiments, the disorder in this alloy is in the SRC limit. These results mandate that Kondo disorder be considered before other more fundamental mechanisms for non-Fermi-liquid behavior are invoked.

ACKNOWLEDGMENTS

We are grateful to C. Baines and D. Herlach for their assistance during the experiments; to S. Mock for measuring the susceptibility of our sample of $\text{CeCu}_{5.9}\text{Au}_{0.1}$ between 4 and 300 K; to P. Coleman, D. L. Cox, A. J. Millis, and C. M. Varma for useful comments, and to H. G. Lukefahr for a critical reading of the manuscript. This research was supported in part by the U.S. NSF, Grant Nos. DMR-9418991 (Riverside) and DMR-9400755 (Gainesville), the U.C. Riverside Academic Senate Committee on Research, the Netherlands Stichting FOM, and the Deutsche Forschungsgemeinschaft, and was carried out in part under the auspices of the U.S. DOE.

*Permanent address: Department of Physics, California State University, Los Angeles, CA 90032.

¹D. L. Cox, Phys. Rev. Lett. **59**, 1240 (1987).

²C. L. Seaman, M. B. Maple, B. W. Lee, S. Ghamaty, M. S. Torikachvili, J.-S. Kang, L. Z. Liu, J. W. Allen, and D. L. Cox, Phys. Rev. Lett. **67**, 2882 (1991); J. Alloys Compd. **181**, 327 (1992).

³B. Andraka and A. M. Tsvelik, Phys. Rev. Lett. **67**, 2886 (1991).

⁴A. M. Tsvelik and M. Reizer, Phys. Rev. B **48**, 9887 (1993).

⁵R. N. Bhatt and D. S. Fisher, Phys. Rev. Lett. **68**, 3072 (1992); V. Dobrosavljević, T. R. Kirkpatrick, and G. Kotliar, *ibid.* **69**, 1113 (1992).

⁶B. Andraka and G. R. Stewart, Phys. Rev. B **47**, 3208 (1993).

⁷H. v. Löhneysen, T. Pietrus, G. Portisch, H. G. Schlager, A. Schröder, M. Sieck, and T. Trappmann, Phys. Rev. Lett. **72**, 3262 (1994).

⁸See, e.g., A. Schenck, *Muon Spin Rotation Spectroscopy* (Adam Hilger, Bristol, 1985).

⁹W. D. Wu, A. Keren, L. P. Le, G. M. Luke, B. J. Sternlieb, Y. J. Uemura, C. L. Seaman, Y. Dalichaouch, and M. B. Maple, Phys. Rev. Lett. **72**, 3722 (1994).

¹⁰A. Amato, R. Feyerherm, F. N. Gygax, A. Schenck, H. v. Löhneysen, and H. G. Schlager, Phys. Rev. B **52**, 54 (1995).

¹¹O. O. Bernal, D. E. MacLaughlin, H. G. Lukefahr, and B. Andraka, Phys. Rev. Lett. **75**, 2023 (1995).

¹²As calculated in Ref. 11, $P(T_K)$ exhibits a logarithmic singularity at $T=0$. It can be seen in Fig. 1, however, that the weight of this singularity is negligible.

¹³E. Miranda, V. Dobrosavljević, and G. Kotliar (unpublished).

¹⁴M. C. Aronson, R. Osborn, R. A. Robinson, J. W. Lynn, R. Chau, C. L. Seaman, and M. B. Maple, Physica B **206&207**, 108 (1995); Phys. Rev. Lett. **75**, 725 (1995).

¹⁵That is, transverse to the muon spin direction.

¹⁶R. S. Hayano, Y. J. Uemura, J. Imazato, N. Nishida, T. Yamazaki, and R. Kubo, Phys. Rev. B **20**, 850 (1979).

¹⁷A. Murasik, S. Ligenza, and A. Zygmunt, Phys. Status Solidi A **23**, K163 (1974).

¹⁸O. O. Bernal, D. E. MacLaughlin, H. G. Lukefahr, and B. Andraka, Physica B **206&207**, 62 (1995).

¹⁹We use the term “local moment” to describe the paramagnetism of these systems even deep into the heavy-fermion state ($T \ll T_K$), since the spin polarization density is expected to be close to that of the atomic (U or Ce) wave function.

²⁰R. E. Walstedt and L. R. Walker, Phys. Rev. B **9**, 4857 (1974).

²¹S. R. Barth, H. R. Ott, F. N. Gygax, A. Schenck, T. M. Rice, and Z. Fisk, Hyperfine Interact. **31**, 397 (1986); S. R. Barth, H. R. Ott, F. N. Gygax, B. Hitti, E. Lippelt, and A. Schenck, J. Magn. Mater. **76&77**, 455 (1988); A. Schenck, P. Birrer, Z. Fisk, F. N. Gygax, B. Hitti, E. Lippelt, H. R. Ott, and M. Weber, Hyperfine Interact. **64**, 511 (1990).

²²O. O. Bernal, Ph.D. dissertation, University of California, Riverside, 1994.

²³A. Schenck, in *Frontiers in Solid State Sciences (Magnetism)*, edited by L. C. Gupta and M. S. Murani (World Scientific, Singapore, 1993), p. 343.

- ²⁴A. Amato, R. Feyerherm, J. Flouquet, F. N. Gygax, P. Haen, D. Jaccard, P. Lejay, H. R. Ott, A. Schenck, J. Sierro, and E. Walker (unpublished).
- ²⁵The five crystallographically inequivalent Cu sites in the unit cell of CeCu₆, together with the different NMR shifts and quadrupole splittings expected for each site and the presence of two Cu isotopes, yield a very complex Cu NMR spectrum. Preliminary measurements on a field-aligned powder sample of CeCu₆ [H. G. Lukefahr (private communication)] have given promising results, however, and NMR studies of CeCu_{6-x}Au_x will be undertaken in the future.
- ²⁶H. G. Schlager, A. Schröder, M. Welsch, and H. v. Löhneysen, *J. Low Temp. Phys.* **90**, 181 (1993).
- ²⁷H. G. Lukefahr, O. O. Bernal, D. E. MacLaughlin, C. L. Seaman, and M. B. Maple, in *Random Magnetism and High-Temperature Superconductivity*, edited by W. P. Beyermann, N. L. Huang-Liu, and D. E. MacLaughlin (World Scientific, Singapore, 1994), p. 101; *Physica B* **199&200**, 413 (1994).
- ²⁸C. Pfeleiderer, G. J. McMullan, and G. G. Lonzarich, *Physica B* **199–200**, 634 (1994).
- ²⁹F. M. Grosche, C. Pfeleiderer, G. J. McMullan, G. G. Lonzarich, and N. R. Bernhoeft, *Physica B* **206-207**, 20 (1995).